

Effects of Al and Co Promoters on CuO/SBA-15/Kaolinite Catalyst Properties and CO₂ Hydrogenation at Low Pressure

Zane Abelniece^{1*}, Valdis Kampars¹, Helle-Mai Piirsoo², and Aile Tamm²

¹Riga Technical University, Institute of Applied Chemistry, Paula Valdena Str. 3, Riga LV-1048, Latvia

²University of Tartu, Institute of Physics, W. Ostwaldi Str. 1, Tartu 50411, Estonia

Abstract. CuO on mesoporous silica catalyst was prepared with post synthesis impregnation method, and the effects of Al and Co promoters on CuO/SBA-15/kaolinite catalyst properties and CO₂ hydrogenation were studied. The mixing technology with kaolinite clay (containing Al₂O₃) was used to obtain the granules and to enhance the CO₂ conversion to methanol as a product. The performance of all catalysts for catalytic hydrogenation of CO₂ was evaluated on a fixed-bed tubular micro-activity reactor at 20 bar and 250°C with H₂/CO₂ molar ratio 3:1. XRD analysis, N₂ adsorption-desorption analysis and SEM-EDX analysis indicated that the mesoporous structure of SBA-15 remains after loading with CuO and promoters, and after mixing with kaolinite clay. Results were compared with results obtained with commercial CuO/Al₂O₃ catalyst, which showed high MeOH selectivity (78%) during CO₂ hydrogenation reaction.

1 Introduction

Fossil fuel depletion, global warming, climate change, and steep hikes in the price of fuels are driving scientists to investigate on commercial and environmentally friendly fuels [1]. Carbon dioxide (CO₂) has been considered as one of the main greenhouse gases, and its increasing emissions arguably lead to the global warming and climate changes [2]. At the same time, CO₂ can be not only a harmful product but also a valuable raw material. However, only a few industrial processes have utilized CO₂ as raw material to produce high-value chemicals. The biggest challenge is the activation of CO₂, which requires large amounts of energy (because of its molecular stability) due to the lack of effective catalysts. Hence, it is essential to develop high-performance catalysts to activate and convert CO₂ under mild conditions [3].

CO₂ catalytic hydrogenation to methanol (MeOH) has been recognized as one of the most effective and economical ways to fix and utilize the emitted CO₂ [2, 4].

Although many kinds of metal-based catalysts have been investigated and examined for the methanol synthesis, copper (Cu) remains the main active catalyst component, together with different promoters [1,4,5,6].

The most active Cu-based catalysts are prepared by a co-precipitation method, and are composed of Cu, ZnO and Al₂O₃ [7, 8]. The addition of metal oxide promoters could increase the catalytic activity by changing the structure and properties of the catalyst [9].

Another factor affecting the performance of catalysts besides active components and promoters, are supports. Several studies have shown that the mesostructured silica SBA-15 (Santa Barbara Amorphous or mesoporous silica) has good application prospects as a

catalyst carrier material because of its flexible pore structure and large specific surface area [9]. With the confinement of the active metal-oxide phase into the mesoporous channels of SBA-15 the nanostructured oxide would be sinter-resistant as well as showing superior metal dispersion [10].

To obtain the granules of catalyst, a kaolinite clay was chosen as binder. It is known that kaolinite contain of quartz and- a lot of Al₂O₃ (35%), and also some metal oxides, that could enhance the CO₂ conversion to methanol [11].

The effects of Al and Co as promoters were studied on CO₂ hydrogenation reaction at 20 bar 250 °C with H₂/CO₂ molar ratio 3:1 for 50 hour. To compare the reaction progress, commercial CuO/Al₂O₃ catalyst was tested on CO₂ hydrogenation reaction at the same conditions.

2 Materials and methods

2.1. Preparation of catalysts

SBA-15 was purchased from ACS Material LLC. Cu(NO₃)₂·2.5H₂O, Al(NO₃)₃·9H₂O, Co(NO₃)₂·6H₂O and ethanol were purchased from Sigma-Aldrich. All chemicals were analytical grade and were used without further purification. Commercial Copper (II) oxide on alumina (CuO/Al₂O₃) 14-20 mesh, 13 wt.% loading were purchased from Sigma-Aldrich.

4.4 g of the SBA-15 was immersed in an ethanol solution containing 4.82 g of Cu(NO₃)₂·2.5H₂O and stirred for 2 h, followed by ethanol evaporation. The solid was calcined at 500 °C for 5h and when 30%CuO/SBA-15 catalyst was mixed with the kaolinite

* Corresponding author: Zane.Abelniece@rtu.lv

clay in a mass ratio of 2:1 using a pestle. Thereafter water was added and the resulting paste was squeezed through a syringe's needle (1.6 mm diameter) to make small cylindrical bodies. After drying the obtained cylindrical bodies were cut into approximately 5 mm length. These granules were calcined and denoted as 20%CuO/SBA-15/Kaolin or C.

One part of the 30%CuO/SBA-15(2g) was immersed in an ethanol solution containing 1.47 g of $\text{Al}(\text{NO}_3)_3 \cdot 9\text{H}_2\text{O}$ and the other part of 30%CuO/SBA-15(2g) in an ethanol solution containing 0.54 g of $\text{Co}(\text{NO}_3)_2 \cdot 6\text{H}_2\text{O}$ and stirred for 2 h, followed by ethanol evaporation. The solid was calcined and mixed with the kaolinite clay following the same procedure as previously. Accordingly, 3%Al/20%CuO/SBA-15/Kaolin or C-Al and 3%Co/20%CuO/SBA-15/Kaolin or C-Co were obtained.

2.2 Characterization of catalysts

Powder crystal phase, i.e., structural analysis was made by X-ray diffractometer (D8 ADVANCE by Bruker AXS GmbH) using 40 kV, 40 mA, Cu $K\alpha$ radiation. Small-angle X-ray diffraction (XRD) patterns were recorded over the range $0.5^\circ \leq 2\theta \leq 2^\circ$ with the step size of 0.01° and over the range $2^\circ \leq 2\theta \leq 50^\circ$ with the step size of 0.02° .

The surface area and the pore size were determined by N_2 adsorption-desorption isotherms obtained at -196°C using a Quantachrome Instruments Nova 1200 E-Series surface and porosity analyzer. The samples were out-gassed at 150°C for 24 h before measurement. Total surface area was estimated by using the Brunauer-Emmett-Teller (BET) method. Pore diameters were derived from desorption isotherms using the Barrett-Joyner-Halenda (BJH) method.

Morphologia and composition were studied using scanning electron microscope (SEM) (Helios Nanolab 600 by FEI). Elemental composition of uncoated samples was determined with energy dispersive x-ray (EDX) analysis detector (INCA Energy 350 by Oxford Instruments).

2.3 Catalyst testing

The CO_2 hydrogenation was performed in a fixed-bed stainless steel tubular micro-activity reactor (Microactivity-Effi, PID Eng&Tech S.L.). For each experiment, 0.70 g of catalyst was loaded in a catalyst bed. The catalysts were reduced *in situ* at atmospheric pressure under a flow of H_2 at flow rate of 50 mL min^{-1} at 350°C for 4 h. After the reduction step, the temperature was lowered to 160°C ; subsequently a flow of H_2 (99.995% purity), CO_2 (99% purity) and N_2 (99.9% purity) mixture (3:1:1) was fed through the reactor at a flow rate of 50 mL min^{-1} . The pressure was increased from atmospheric to 20 bar and the temperature in the catalyst bed was increased from 160°C to 250°C at a rate of 2°C min^{-1} . The time on stream after achieving the reaction temperature was 50 h. After leaving the reactor,

the exit gas passed through cold trap ($T=5^\circ\text{C}$) to condense products.

The reactor outlet gas composition was analyzed on-line by a gas chromatograph (Shimadzu Nexis GC-2030) equipped with four columns, flame ionization detector (FID) and thermal conductivity detector (TCD) with helium as carrier gas. $250\ \mu\text{L}$ of sample at normal pressure was injected using sample loop. Multicolumn chromatography system consisting of two Restek Porapak Q 80/100 (6 ft, 2 mmID) and Restek Molesieve 5A 60/80 (6 ft, 2 mmID) columns and TCD detector were used for the analysis of gases.

The CO_2 conversion (X) and product selectivity (S) is calculated as follows:

$$X_{\text{CO}_2} = \left(\frac{n\text{CO}_2_{\text{in}} - n\text{CO}_2_{\text{out}}}{n\text{CO}_2_{\text{in}}} \right) \times 100 \quad (1)$$

$$S_i = \left(\frac{A_i}{\sum A_i} \right) \times 100 \quad (2)$$

where $n\text{CO}_2_{\text{in}}$ and $n\text{CO}_2_{\text{out}}$ is the number of moles of CO_2 at the inlet and outlet, respectively. A_i and $\sum A_i$ represent the mole of selected product 'i' and total mole of all product.

3 Results and discussion

Small-angle XRD patterns of all CuO/SBA-15 samples (Fig. 1 A) exhibited (100), (110), and (200) diffraction reflection representing two-dimensional hexagonal mesoporous structure [12].

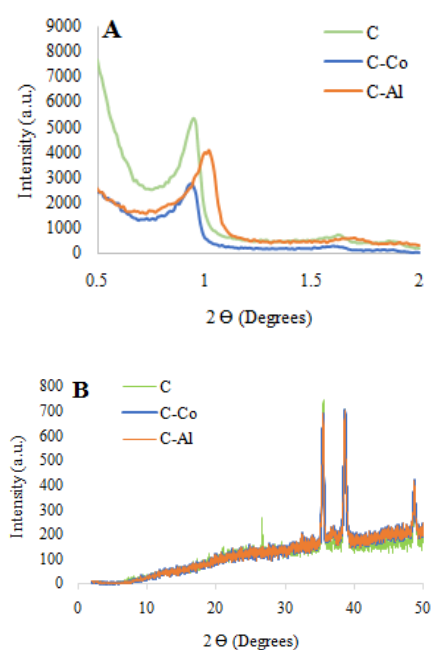


Fig. 1. Small-angle XRD (A) and wide-angle XRD (B) patterns of CuO/SBA-15 samples.

It indicates that the Cu, Al and Co loading and the mixing technology with clays did not damage the structure.

Wide-angle XRD pattern (Fig. 1 B) exhibited peaks at 2θ of 35.5° , 38.8° and 48.8° , which correspond to (002), (111) and (-202) planes of CuO tenorite phase (PDF 01-073-6023) [13]. From this it can be concluded that the calcination in air for 5 h at 500°C produced a relatively pure phase of supported CuO on SBA-15.

Fig.2. exhibits UPAC type IV isotherms with a H1 hysteresis loop for all CuO/SBA-15 catalysts, corresponding to the mesoporous materials consisting of ordered array of cylindrical pores [14], which indicates that the mesoporous structure of SBA-15 was not damaged after metal loading and mixing with kaolinite. N_2 adsorption-desorption isotherm of commercial CuO/ Al_2O_3 catalyst exhibits UPAC type IV isotherm with a H3 hysteresis loop, corresponding to the mesoporous materials [15]. Fig. 3. shows, that C and C-Co catalysts exhibited the uniform pore size distribution (average diameter 6.6nm), C-Al catalyst exhibited bimodal pore size distribution (6.6 and 3.9 nm), that could be explained by Al loading on the walls of some of the pores. CuO/ Al_2O_3 catalyst has no uniform pore size distribution.

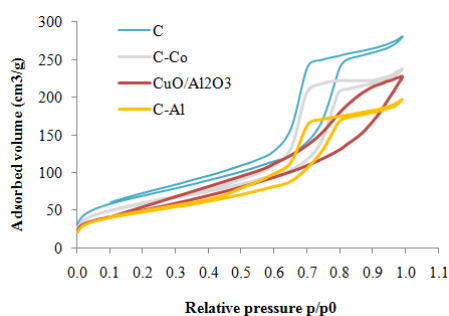


Fig. 2. N_2 adsorption-desorption isotherms.

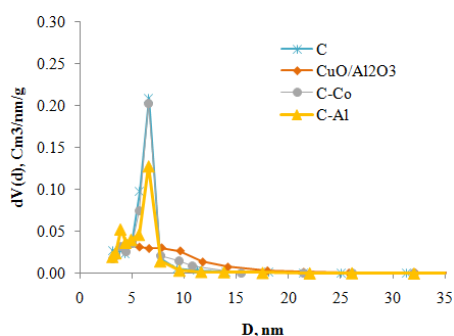


Fig.3. Pore size distribution of catalysts.

As shown in Table 1, the surface area and the volume of pores of C-Al and C-Co catalysts are smaller than surface area and the volume of pores of C catalyst, due to additional metal loading on mesoporous silica. Surface reduction is observed due to filled pores. Commercial CuO/ Al_2O_3 catalyst's surface area is slightly smaller than the surface area of others - CuO/SBA-15 catalysts.

Table 1. Structural properties of catalysts.

Catalyst	BET surface area [m^2/g]	Dpore [nm] ^a	Vtotal [cm^3/g] ^b
CuO/ Al_2O_3	185.6	4.98	0.35
C	247.5	6.63	0.43
C-Al	172.6	6.61	0.31
C-Co	209.3	6.60	0.37

^a Pore diameter was derived from the desorption branches of the isotherms by using the BJH method.

^b Total pore volumes were estimated from the absorbed amount at a relative pressure of $p/p_0 = 0.99$

As explored in our previous work, 30 wt.% Cu amount loading on mesoporous silica with post-impregnation method resulted in a catalyst with large particle agglomerates. EDX results confirm very high concentration of Cu in these agglomerates – even 58% (catalyst C-Co), see Table 2. It is known that kaolinite clay contains 35% Al_2O_3 [11], thereby in results Al appears in all samples. Also, a small amount of Fe and Ti were found in some of samples indicating to the additives in the clay. Co content in these agglomerates reaches 2% and Al content reaches 8%, though Al content is higher than amount loaded because of kaolinite co-mixing. Co and Al were dispersed regularly on the SBA-15 surface, however their content in agglomerates is lower than on regular surface, see Table 2. The content of Cu in CuO/ Al_2O_3 catalyst matches with content specified by the manufacturer.

Table 2. EDX analysis of catalysts.

Catalyst	Spectrum area*	Chemical element, weight %					Other (Fe, Ti)
		O	Al	Si	Co	Cu	
CuO/ Al_2O_3	r	46.48	40.62			12.9	
	a	31.19	3.2	9.79		55.82	
C	r	49.39	7.49	42.12		1.00	
	r	55.62	6.87	32.61		4.03	0.87
	a	30.86	1.37	7.4	1.95	58.42	
C-Co	r	57.33	3.1	34.97	3.29	1.05	0.27
	r	53.82	4.12	32.55	4.88	4.28	0.35
	a	36.89	8.07	10.93		44.12	
C-Al	r	56.7	11.5	26.65		5.15	
	r	56	10.61	26.89		6.24	0.26
	a	36.89	8.07	10.93		44.12	

* Spectrum of agglomerates - a or spectrum of regular areas - r

The CO_2 conversion of hydrogenation reaction exceeded 10% with C-Co catalyst. The CO_2 conversion with other catalysts did not exceed 5% that may be explained by insufficient amounts of small particles due to agglomeration.

10% is typical conversion level for CO_2 hydrogenation by low pressure – 20 bar [16], [17]. In this study, we will focus on the products in the gaseous

phases of reactions, as the methanol in liquid phase was obtained only when commercial Copper (II) oxide on alumina CuO/Al₂O₃ catalyst was used. It showed high enough selectivity (78%) in the gaseous phase.

Catalyst with Co does not show methanol formation, which could thus be used for another purpose. As shown in Fig. 4., additional loading of Al and Co as promoters on CuO/SBA-15 showed a negative effect on MeOH formation, on the contrary, the methane content increased, and searches for other promoters are required.

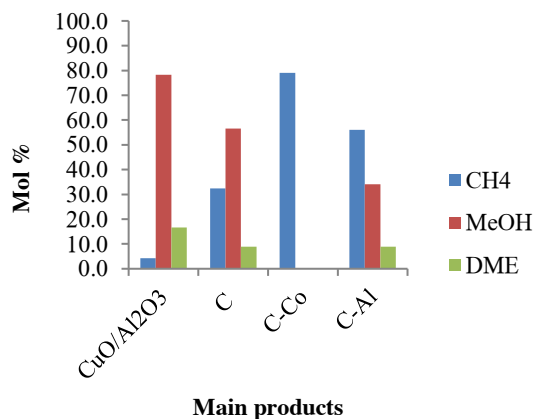


Fig. 4. Influence of catalyst type to distribution of main products in gaseous phase.

4 Conclusion

XRD analysis, N₂ adsorption-desorption analysis and SEM-EDX analysis indicated that the mesoporous structure of SBA-15 remains after loading with CuO and promoters, and after mixing with kaolinite clay.

The highest MeOH selectivity (78%) during CO₂ hydrogenation reaction at 20 bar and 250°C with H₂/CO₂ molar ratio 3:1 was observed with commercial Copper (II) oxide on alumina CuO/Al₂O₃ catalyst. Additional loading of Al and Co as promoters on CuO/SBA-15 showed a negative effect on MeOH formation, on the contrary, the methane content increased, and searches for other promoters are required.

This work has been supported by the European Regional Development Fund within the Activity 1.1.1.2 “Post-doctoral Research Aid” of the Specific Aid Objective 1.1.1 “To increase the research and innovative capacity of scientific institutions of Latvia and the ability to attract external financing, investing in human resources and infrastructure” of the Operational Programme “Growth and Employment” (No.1.1.1.2/VIAA/3/19/396).

The study was partially supported by the Estonian Research Agency project PRG4 and the European Regional Development Fund project “Emerging orders in quantum and nanomaterials” (TK134).

References

1. S. Saeidi, N. A. S. Amin, and M. R. Rahimpour, J. CO₂ Util., vol. **5**, pp. 66–81 (2014) doi: 10.1016/j.jcou.2013.12.005
2. J.-Y. L. Hong Ren, Cheng-Hua Xu, Hao-Yang Zhao, Ya-Xue Wang, Jie Liu, J. Ind. Eng. Chem., vol. **25**, pp 261-267 (2015)
3. B. L. D. Venkata, D.B.C. Dasireddy, Renew. Energy, vol. **140**, pp. 452-460 (2019)
4. N. D. Nielsen, A. D. Jensen, and J. M. Christensen, J. Catal., vol. **393**, pp. 324–334, (2021) doi: 10.1016/j.jcat.2020.11.035
5. H. Zhan, X. Shi, B. Tang, G. Wang, B. Ma, and W. Liu, Catal. Commun., vol. **149**, p. 106264, (2021) doi: 10.1016/j.catcom.2020.106264
6. G. Zhang, G. Fan, L. Yang, and F. Li, Appl. Catal. A Gen., vol. **605**, p. 117805 (2020) doi: 10.1016/j.apcata.2020.117805
7. H. W. S. Jun Hu, Yangyang Li, Yanping Zhen, Mingshu Chen, Chinese Journal of Catalysis, vol. **42**, pp. 367–375 (2021)
8. V. L’hospital, L. Angelo, Y. Zimmermann, K. Parkhomenko, and A. C. Roger, Catal. Today, In Press (2020) doi: 10.1016/j.cattod.2020.05.018
9. M. Lin, W. Na, H. C. Ye, H. H. Huo, and W. G. Gao, Journal Fuel Chem. Technol., vol. **47**, no. 10, pp. 1214–1225 (2019) doi: 10.1016/s1872-5813(19)30048-9
10. M. Mureddu, F. Ferrara, and A. Pettinau, Appl. Catal. B Environ., vol. **258**, pp.117941 (2019) doi: 10.1016/j.apcatb.2019.117941
11. Q. Mohsen and A. El-maghraby, Arab. J. Chem., vol. **3**, no. 4, pp. 271–277 (2010) doi: 10.1016/j.arabjc.2010.06.015
12. D. Zhao *et al.*, “Triblock copolymer syntheses of mesoporous silica with periodic 50 to 300 angstrom pores,” Science (80-.), vol. **279**, no. 5350, pp. 548–552, (1998) doi: 10.1126/science.279.5350.548
13. “<https://rruff.info/Tenorite/R120076>.”
14. Z. A. Alothman, “A review: Fundamental aspects of silicate mesoporous materials,” Materials (Basel), vol. **5**, no. 12, pp. 2874–2902 (2012) doi: 10.3390/ma5122874
15. K. S. Sing, W. D. H. Everett, R. A. W. Haul, L. Moscou, R. A. Pierotti, J. Rouquerol, Pure Appl. Chem., vol. **57**, no. 4, pp. 603–619 (1985)
16. M. K. Koh, M. M. Zain, and A. R. Mohamed, “Exploring transition metal (Cr, Mn, Fe, Co, Ni) promoted copper-catalyst for carbon dioxide hydrogenation to methanol,” AIP Conf. Proc., vol. **2124** (2019) doi: 10.1063/1.5117066
17. A. M. Z. Noor, T. Sara, and S. S. Maizatul, Key Eng. Mater., vol. **708**, pp. 94–97 (2016) doi: 10.4028/www.scientific.net/KEM.708.94